MANCHESTER 1824
The University of Manchester

The University of Manchester Research

Testing different supervised machine learning architectures for the classification of liquid crystals

DOI:
10.1080/02678292.2023.2221654

Document Version
Accepted author manuscript

Link to publication record in Manchester Research Explorer

Citation for published version (APA):
Dierking, I., Dominguez, J., Harbon, J., & Heaton, J. (2023). Testing different supervised machine learning architectures for the classification of liquid crystals. *Liquid Crystals*. https://doi.org/10.1080/02678292.2023.2221654

Published in:
Liquid Crystals

Citing this paper
Please note that where the full-text provided on Manchester Research Explorer is the Author Accepted Manuscript or Proof version this may differ from the final Published version. If citing, it is advised that you check and use the publisher's definitive version.

General rights
Copyright and moral rights for the publications made accessible in the Research Explorer are retained by the authors and/or other copyright owners and it is a condition of accessing publications that users recognise and abide by the legal requirements associated with these rights.

Takedown policy
If you believe that this document breaches copyright please refer to the University of Manchester's Takedown Procedures [http://man.ac.uk/04Y6Bo] or contact uml.scholarlycommunications@manchester.ac.uk providing relevant details, so we can investigate your claim.

OPEN ACCESS

Download date:04. Sep. 2023

Testing different supervised machine learning architectures for the classification of liquid crystals

Ingo Dierking, Jason Dominguez, James Harbon, Joshua Heaton*

Department of Physics and Astronomy, The University of Manchester, Oxford Road, Manchester M13 9PL, UK

Abstract

Different convolutional neural network (CNN) and inception network architectures were trained for the classification of isotropic, nematic, cholesteric and smectic liquid crystal phase textures to test the prediction accuracy for each one of these models. Varying the number of layers and inception blocks, as well as the regularization, and application to different phase transitions and classification tasks, it is shown that in general the architecture of an inception network with two blocks leads to the best classification results. Regularization, such as image flipping, and dropout layers additionally somewhat increases the classification accuracy. Even for simple tasks like the isotropic-nematic transition, which is of importance for applications in the automatic readout of sensors, convolutional neural networks need more than one layer. Care must be taken to not apply architectures of too large complexity, as this will again reduce the classification accuracy due to overfitting. Architecture complexity needs to be adjusted to the given classification task.

1. Introduction

1.1 Background and Motivation

Liquid crystals (LCs) are fluids with partial order, thermodynamically located between that of the isotropic and the crystalline phases [1,2]. Whilst perfect crystals have full three-dimensional order and isotropic fluids have none, LC phases have orientational order and sometimes one-, two- or three-dimensional positional order. Thermotropic liquid crystal phases can be categorized into several different classes. The phase with the lowest order and highest symmetry is the nematic, N, phase, which solely exhibits orientational order of the long molecular axis along a preferred direction called the *director*. This phase often shows characteristic topological defects in the form of two or four brushes, called the Schlieren texture [3], which makes it easy to be identified via machine learning. If the nematic phase is chiral, either by inherent chirality due to chiral elements within the molecular structure or through the addition of a chiral dopant, one speaks of the cholesteric, N*, phase. This exhibits a helical superstructure of the director and gives rise to characteristic oily-streaks defects, which are also easily observed in polarized microscopy [3].

Next on cooling, one can observe phases with one-dimensional positional order, thus the formation of smectic layers, the so-called fluid smectic phases, SmA or SmC, depending on whether the director is parallel or tilted to the smectic layer normal, respectively. Both phases often show fan-shaped textures (SmA) or broken fan-shaped textures (SmC) [3]. Also these phases may be chiral with the SmC* phase exhibiting ferroelectric properties and a helical superstructure often visible as a pattern of equidistant lines. Once short range in-plane order is additionally introduced within the smectic layers, we speak of the hexatic phases for the orthogonal phase (SmB) and different tilt direction with respect to the local hexatic order (SmI, SmF), respectively. Hexatic phases also often show fan-shaped textures. Again, these phases can be chiral, yet a helical superstructure is only seldomly observed and is often only partial. Smectic phases with three-dimensional positional order are also known as soft crystal phases. These often exhibit mosaic textures but are usually only very hard to tell apart [3].

To characterize the diversity of liquid crystalline phases with varying degrees of order, several experimental techniques are employed [4]. At first, there is differential scanning calorimetry (DSC) which provides information about transition temperatures, widths of different liquid crystalline phases and the order of phase transitions between different phases, as well as the transition enthalpies. For example, transitions between the isotropic and the LC phases are normally of first order, related to relatively large changes in structure and transition enthalpies, ΔH, in the order of several kJ mol^{-1}. Transitions between fluid smectic phases, for example SmA-SmC, are generally of second order with a vanishing transition enthalpy. DSC will not be able to allow a prediction of the nature of a corresponding phase.

A second method to characterize the phase behavior of liquid crystals is polarized optical microscopy (POM), where a thin sample of the liquid crystal is prepared between untreated glass plates and placed in a hot stage between two crossed polarisers of a microscope. This will produce images of characteristic textures which can, by means of guessing, experience and comparison, be related to

the observed liquid crystal phase [3]. This method can yield the phase transition temperatures and provide a good guess of the observed phase, yet it does not represent proof of a particular molecular arrangement.

A third experimental method, which can in fact lead to the characterization of liquid crystalline order is temperature-controlled X-ray diffraction on oriented samples [4]. It nevertheless should be pointed out, that this methodology is often quite hard to perform and time consuming. It would thus be worthwhile to have a further method at disposal which goes beyond the qualified guesses of POM while being more straight forward than X-ray diffraction. This is where we suggest that machine learning may come in helpful as a method based on POM, yet possibly combining the experience of a whole community of researchers in identifying different phases automatically.

Currently, POM and DSC can be utilized together. POM provides phase and transition temperature information via textures and DSC provides further transition information. We propose to follow on from the work done by Sigaki et al. [5,6], who used machine learning to accurately identify the isotropic and nematic phases from their textures. A machine learning model capable of running with accessible computational power, which can identify LC phases and transitions, would be useful alongside the currently leading techniques. This model would provide benefits over POM in that it would not require extensive LC experience and benefits over DSC in that it would be able to provide information about the phase, as well as the transition temperature.

In the last years, machine learning has found its ways into the design, synthesis and characterization of molecules and materials, and thus also into the prediction of applicational aspects of material science [7,8]. With soft condensed matter being on the rise in materials science this trend has obviously not stopped short for the design and property prediction of soft materials [9] of which liquid crystals are an integral part. It is therefore not surprising that first publications of machine learning in liquid crystals have been published very recently, although the field is still in its infancy. Most of these publications are concerned with the prediction of properties such as phases and phase transition temperatures of liquid crystals [5,6,10,11]. A focus has so far been the isotropic to nematic transition of thermotropics, using both simulated as well as experimental data. But also polydisperse systems [12] as well as lyotropic liquid crystals [13] have been investigated. A lot of the work so far has been related to nematic topological defects in one way or the other, which may be formed in the presence of planar boundary conditions in the form of the above mentioned Schlieren textures. Classifications of these defects have been carried out on simulated data [14] as well as on experimental textures [15]. A particularly interesting investigation was carried out in the study of hydrodynamics of active nematics [16], which display such topological defects. Other work has used machine learning in the detection and tracking of circular inclusions (islands, droplets, bubbles) in free-standing smectic films [17] which then allows an investigation of convection properties.

All such machine learning studies are of course relevant for the application of liquid crystals in a range of different devices. The identification of Blue Phases [18,19] can for instance enable novel mixtures for BP displays. A further field is the exploitation of liquid crystals in chemical and biological sensors [20]. In principle, these all use the transition from homeotropic to planar orientation, thus a director field reorientation from a uniformly black to a bright state, again with the exhibition of topological defects, which allows the automatic readout via machine learning [21]. This has also been

demonstrated for gas sensors [22,23], SARS-CoV-2 by use of a viral induced texture transition [24], or in the detection of endotoxins from different bacterial species [25]. At last, machine learning has also been employed in medicine, via automatic thermography examination for breast cancer using the selective reflection of cholesteric liquid crystals [26]. A rather different application of machine learning in relation to liquid crystals can be found in industrial quality control during the production of TFT-LCD substrates [27-29].

In our investigations we would like to take the analysis of liquid crystal phases to a level beyond the isotropic/pseudo-isotropic to nematic transition by using machine learning algorithms on different transitions, whole phase sequences and to characterize transition temperatures [30,31]. Here, we will test different machine learning architectures, varying algorithms from convolutional networks to inception networks, changing the number of layers and inception blocks, as well as varying the regularization employed and discuss which will be more suitable to different classification tasks.

2. Theory

2.1 Machine Learning

2.1.1 Supervised Machine Learning and Deep Learning

In supervised machine learning there is a set of data, known as training data, for which the expected output, or label, is known [32]. Using this, supervised learning aims to learn the mapping from the inputs to the known outputs [33]. This is known as training a model. An example of this is linear regression. x coordinates and their corresponding y coordinates are known and a mapping, or linear fit, is learned. This can then map new x coordinates to their predicted y values. Within machine learning, deep learning is the current leading technique, being held largely responsible for the rapid advances in machine learning [33].

Artificial neural networks (ANNs) are an example of deep learning. These consist of layers of 'neurons'. The connection of many neurons, which perform different computations, allows for the ANN to model a complex function [34]. The complexity of this function is increased by increasing the number of neurons and or layers in the network [32]. Training an ANN follows the form: forward propagation, backward propagation, weight updates and repetition. For each neuron, i, in the layer l of an ANN, there are associated weights, $\boldsymbol{w}^{[l]}$ [34]. In forward propagation, the ANN is presented with one or more data examples, represented by a feature vector, $\boldsymbol{x}$. For images, $\boldsymbol{x}$ could be the pixel values flattened from a matrix to a column vector. With the input, each neuron, i, computes to

$$\sum_{k=1}^{n} \boldsymbol{w}_{i,k}^{[l]} + \boldsymbol{w}_{i,0}^{[l]} \quad (1)$$

[32]. A non-linear function is then applied to this value. A common choice is the rectified-linear-unit (ReLU) function, which is zero for arguments below zero and linear for those above zero. The outputs of neurons in one layer are the input to each neuron in the next layer. This continues until the last output layer is reached. Each neuron in this layer computes an output, or prediction, $y_{pred,i}$. With the

output of the network, the loss is calculated. For classification problems, a commonly used loss function is the categorical cross-entropy loss, which is

$$L = -\sum_{i=1}^{N} y_i \log y_{pred,i} \quad (2)$$

[32] for a single example input. Here, y_i is the expected output and the sum is over each output neuron of the network, N, the number of prediction classes. For an output layer with three neurons, an output could be $[y_{pred,1},\ y_{pred,2},\ y_{pred,3}] = [0.2, 0.1, 0.7]$. An example of an expected output could be $[y_1,\ y_2,\ y_3] = [0, 0, 1]$, representing the third class in this three-class classifier. The backpropagation algorithm then uses this loss to update the weights via a gradient-based optimization algorithm, such as gradient descent,

$$\boldsymbol{w}^{[l]} := \boldsymbol{w}^{[l]} - \alpha \frac{\partial L}{\partial \boldsymbol{w}^{[l]}} \quad (3)$$

[34], where α is a predefined learning rate. The Adam algorithm is a commonly used variant of gradient descent, changing the learning rate during training, which has been shown to reach convergence sooner than standard gradient descent [35]. The entire process is repeated until the loss, which is inversely related to accuracy, is lowered to convergence.

2.1.2 Bias-Variance Tradeoff and Generalizability

When applying deep learning to a dataset it is common practice to have a training set and test set. The methodology is that a model is trained using the training set examples and then applied to the test data to evaluate if the model generalizes to unseen data [33].

One problem faced in the training of a model is the bias-variance tradeoff, also known as under or overfitting. A model can overfit to the training data, meaning it has high variance and low bias. This is seen by a high training accuracy and a lower test accuracy [32]. Figure 1 shows an example of this, where a model has learned to recognize the noise in training data. This will not generalize sufficiently well to unseen data. Alternatively, if the training accuracy is lower than desired, the model is said to underfit the training data - low variance, high bias [33]. The ideal model will achieve a test accuracy as high as possible, depending on the difficulty of the task.

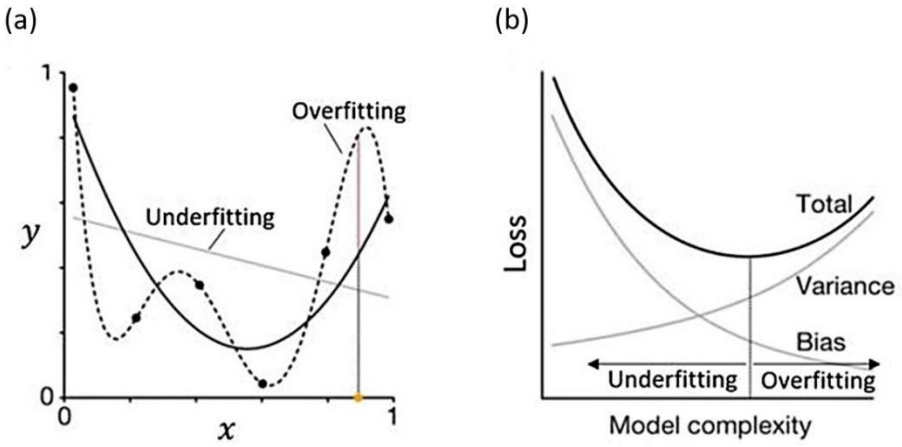

Figure 1: (a) Effects of under and overfitting and (b) how loss can indicate this. In (a), using a linear function (grey) to fit a quadratic data functionality (solid black) would indicate underfitting, while using a higher polygon

(dashed black) would imply overfitting. This illustrates that in machine learning it is important to adjust the complexity of the architecture to the classification task. Figure edited from [36].

A validation set of data is often used during training. This is a small portion of the training data which is held-out and not used for updating weights. For every epoch, which is an iteration through all the training data, the accuracy on the validation set is computed. Monitoring this accuracy can identify when the model is overfitting training data, as the validation accuracy will be lower than the training accuracy. Using this information, hyperparameters of the model, such as number of layers, can be changed [33].

2.2 Convolutional and Inception Networks

Figure 2(a) shows the general architecture of a convolutional neural network (CNN). CNNs are a type of ANN which perform better for image classification problems. They include convolutional and subsampling layers, before the output is flattened into a vector and passed through an ANN [37]. Convolutional layers have filters of a certain size and perform convolutions over the entire area of the input. Rather than having weights to update, convolutional layers update the parameters in the filters [32].

Subsampling, or pooling layers look at a certain sized area of the input and then output the maximum value in that area [32]. They thus down sample the feature maps by summarizing the features in patches of the feature map. There are no trainable parameters in pooling layers, so they help to reduce the computational cost of a CNN and also reduce the problem of overfitting.

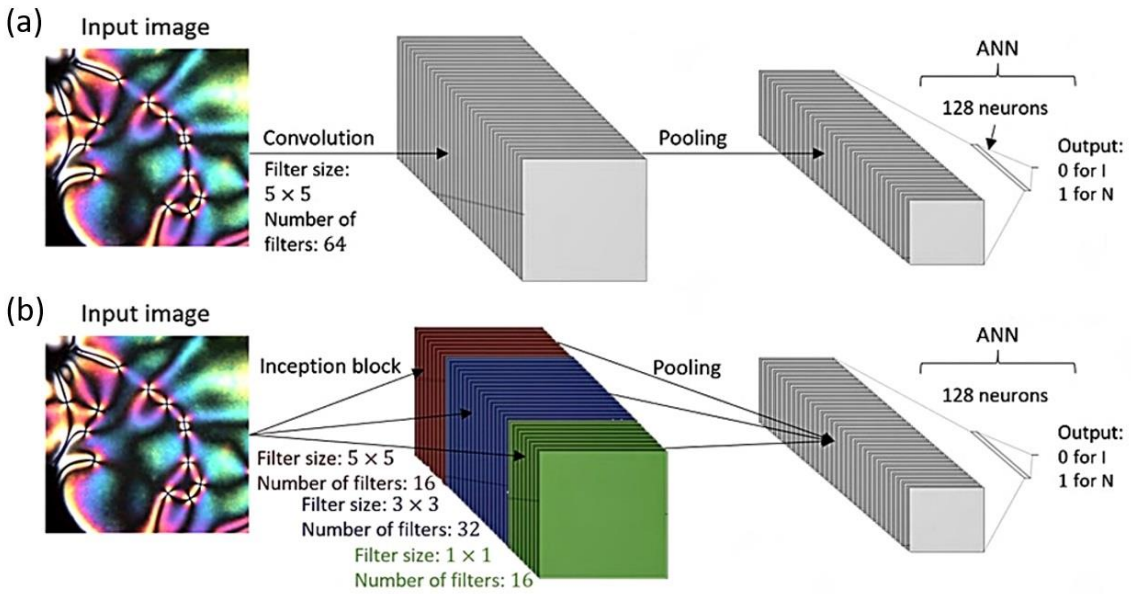

Figure 2: Summary of the general architecture of (a) a convolutional neural network and (b) an inception network.

In 2014, researchers at Google designed GoogLeNet, an Inception network, which achieved the highest accuracy in the 2014 ImageNet image classification competition [38]. Inception networks

replace the convolutional layers in CNNs with Inception modules, as shown in Figure 2(b). The Inception module utilizes layers with different properties, such as filter size, or type, in parallel. One benefit of this is that it removes the need to guess what layer should be used [38]. Instead, by having different layers in parallel, the network can learn which layer is best suited, through the training process. Having different layers in parallel is computationally very expensive, so to mitigate this, 1×1 convolution layers are often used to reduce the number of computations performed [38].

3. Collection and Preparation of Texture Images

Before the implementation of a supervised deep learning model, POM texture images, grouped by phase, and transition videos needed to be collected. The complete dataset obtained consists of 11773 textures of different phases. In particular, these were 1981 isotropic, 2813 nematic, 2132 cholesteric (chiral nematic), 1284 SmA, 1448 SmC, 396 SmI, 270 SmF images, as well as 945 images of an unidentified soft crystal phase and 504 images of the crystalline phase. The images used were obtained from POM phase transition videos of the 5CB, 8CB, D5 to D9 [39] and M6 to M10 [40] liquid crystals.

To get images from the videos, the open-source VLC media player [41] was used to extract the frames from the videos. Frames were captured every five to twenty frames depending on how fast changes occurred in the video. Having many, almost identical, images would take up more storage space and have little benefit for a deep learning model. The images obtained from these videos had a resolution of 2048 × 1088. As this was a large resolution, the images were then split into six 682 × 544 images, increasing the total number of different images in the dataset to that mentioned above. This resolution still allowed key features of the textures to be identified. Figure 3 shows a summary of the image preprocessing applied for convolutional neural networks and inception networks.

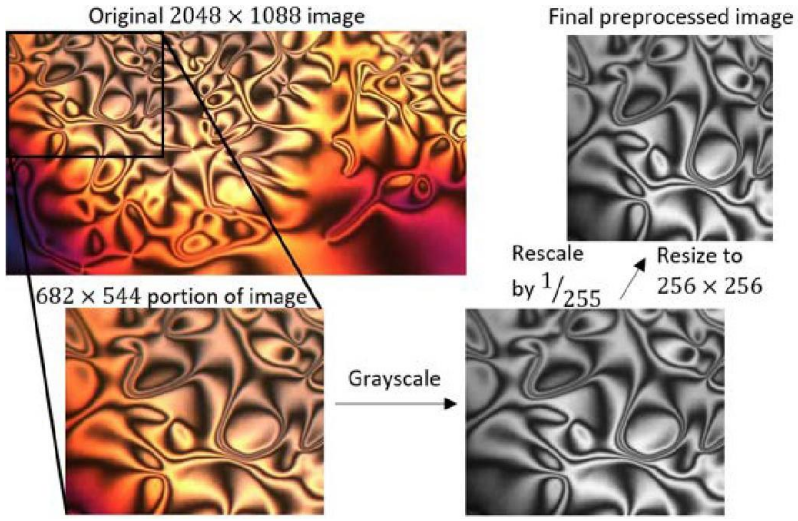

Figure 3: Diagrams of all the images pre-processing steps performed on an example nematic texture before use in a deep learning model.

The videos, from which the images were extracted had known phases, phase transition temperatures and temperature ranges so that the phase of the images could be identified. Images of the liquid crystals D5 to D8 and M6 to M10 were grouped using transition temperature information from POM and literature [39,40]. Images from the 5CB and 8CB LCs were identified by POM as they exhibited visually distinct isotropic, nematic and smectic phases. All images of a single phase were grouped in the same folder and stored.

The Keras deep learning framework [42] in Python was used to implement deep learning models. In all these models, real-time preprocessing was done via Keras. Images were converted to grayscale. This was done because texture, rather than color, determines the phase and because computational time can be saved. Images were further resized to 256 × 256 to obtain square images of dimensions that are powers of two. Both of these scalings are common practices with CNNs [32]. Further, this image size was small enough to reduce the computation time for working with standard personal computers, without obscuring texture details. Finally, the image's grayscales were rescaled by 1/255, so that pixel values were between 0 and 1, a requirement for CNNs to work correctly [32].

4. Data Selection and Training Image Classification Models

4.1 Isotropic, Nematic, Cholesteric and Smectic Phase Classification

4.1.1 Method

The first attempt at applying machine learning to LC phase transitions was performed for phase transitions involving the isotropic, nematic, cholesteric or smectic phases, as these are the easiest to distinguish visually. To achieve this, an isotropic, nematic, cholesteric and smectic image classifier needed to be trained.

Before training a model, it was necessary to create training and validation image sets and a test set of phase transition videos. The videos selected for the test set were those of the 8CB and the liquid crystal M6, as these involved a variety of different transitions between the phases. To avoid data leakage, where a model has effectively 'seen' the answer before, any images extracted from these videos were not included in the training or validation sets. Images from a single video were not split between training and validation, again to avoid data leakage. Further, the sets were balanced, with a roughly equal number of images of each phase, by deleting similar images from over-represented phases. This was to avoid bias towards predicting one phase.

A training and validation dataset was made which consisted of 1446 training / 259 validation images for the isotropic phase, 1367 / 392 for nematic, 1547 / 352 for cholesteric and 1499 / 543 training vs validation images for the smectic phases. The training- validation split was also approximately 15% validation images and the above mentioned precautions for avoiding data leakage were followed. Using this dataset, CNNs and Inception networks of varying layers were trained for three repeats in order to find the model architecture with the highest validation accuracy. Each model was trained using a default Adam optimizer and categorical-cross entropy loss function. Training was done using a Google Colaboratory [43] GPU, allowing for quicker training times as compared to a standard CPU.

4.1.2 Results

For this classification problem, the training and validation accuracy and loss were computed after each training epoch and plotted, as shown in Figure 4(a) for the convolutional network. One can observe a lot of fluctuation in the validation accuracy and loss. This is possibly due to the relatively small size of the validation set, where a change in prediction for a small number of images can have a larger effect on the accuracy and loss. Overall, this shows that the validation accuracy reached its maximum value at epoch 78 with a value of 69.8%. However, the validation loss is seen to increase. This is usually a sign of overfitting to the training images, also shown by the training accuracy being much higher than the validation accuracy. Figure 4(a) also shows the confusion matrix for this trained model for the validation set images. In the ideal case the model exhibits 1 for every entry in the diagonal, indicating that each image was predicted correctly. From Figure 4(a) it can be seen that this model mislabeled 75.15% of the validation smectic phases as nematic, indicating that it had not learned to distinguish the two.

(a) Convolution model

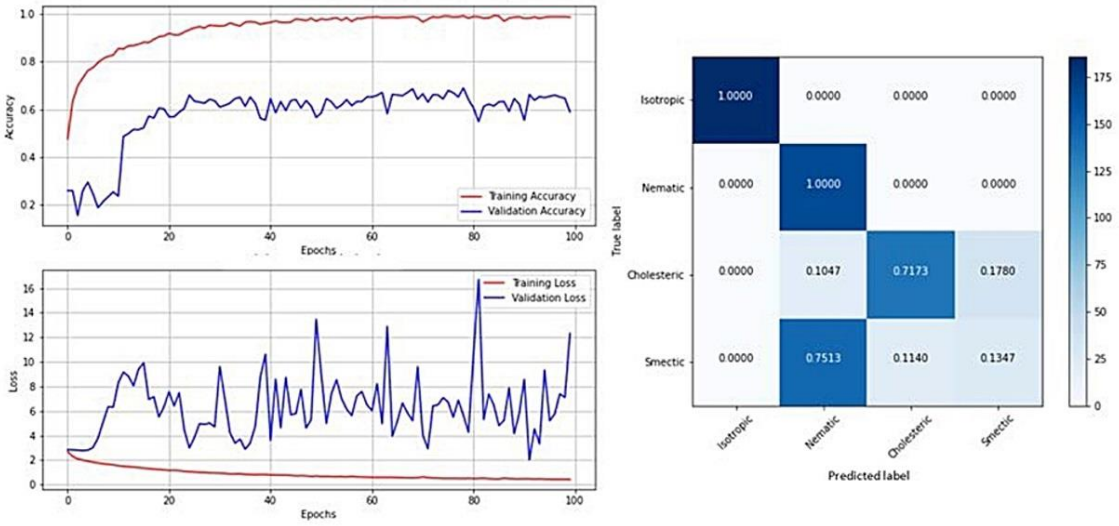

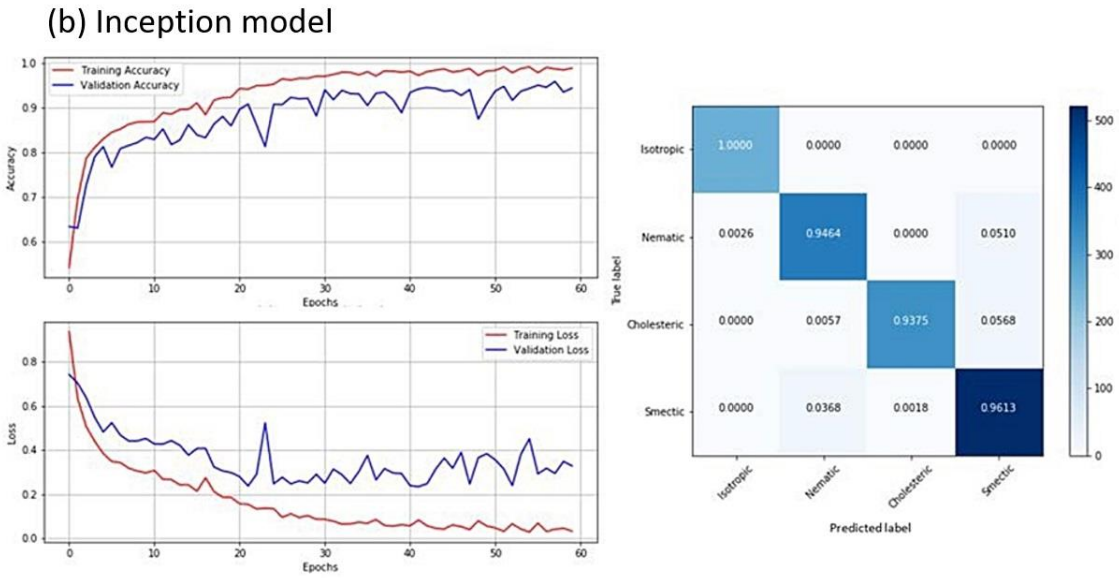

Figure 4: Training (red) and validation (blue) accuracy and loss as a function of training epochs for (a) convolutional neural network and (b) an inception network of a complex classification task involving isotropic, nematic, cholesteric and smectic textures. Corresponding confusion matrices are also provided which indicate that the CNN architecture does not distinguish between cholesteric and smectic and mislabels these textures. The inception model on the other hand provides excellent results with an average classification accuracy in excess of 94%.

From attempts to increase the number of layers it can be seen that, for CNN models, increasing the number of layers increased the validation accuracy (see also below). Overall, Inception networks achieved a higher accuracy, as is also depicted in figure 4(b) where the highest validation accuracy, of 95.9% was achieved. With a training time per epoch of 90 s, the total training time was approximately 1.5 hours. The model also showed less overfitting to the training data than most models. This can be seen in Figure 4(b), as its loss is mostly decreasing. The confusion matrix for the inception model shows that all phases were correctly predicted from textures, with a high accuracy achieved. Overall, the inception model showed a more accurate performance on the unseen validation images than the convolutional neural networks.

4.2 Fluid Smectic and Hexatic Phase Classification

4.2.1 Method

For creating a classifier to identify transitions between fluid smectic and hexatic phases, the first step was again to create an image classifier. Due to its high accuracy on the previous task, the Inception model architecture was used. The output had to be change from a four-class to binary output. Because of the small number of fluid smectic and hexatic images, relative to other phases, a dataset containing only fluid smectic and hexatic images was created. This was to avoid having to distinguishing among many phases, including fluid smectic and hexatic. The training set consisted of 777 fluid smectic textures and 516 hexatic textures. The validation set consisted of 114 and 102 fluid smectic and hexatic textures, respectively. Fluid smectic images were comprised of a roughly equal number of SmA and SmC images, whereas the hexatic images were comprised of SmF and SmI images

with an approximate ratio of 2 : 3. The same methods to avoid data leakage as outlined above were followed. Only two test videos were chosen, of the D7 and D8 liquid crystals, to avoid further limiting the number of images available for the training and validation sets.

4.2.2 Results

Figure 5 shows the accuracy and loss curves for the inception model applied to this classification problem. At epoch 46, the highest validation accuracy of 98.2%, was achieved. After this epoch, the loss starts to increase, indicating that overfitting was starting to occur. From the confusion matrix for the trained model, it can be seen that predictions of unseen images for each class were highly accurate.

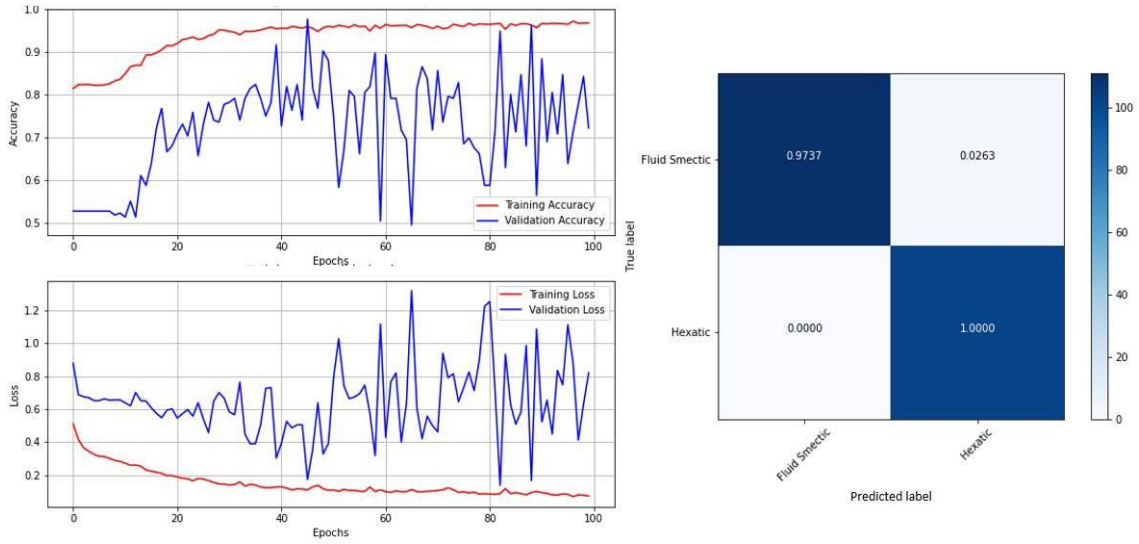

Figure 5: Training (red) and validation (blue) accuracy and loss as a function of epochs for the classification task to distinguish between fluid smectic and hexatic smectic phases via an inception model. The confusion matrix indicates a high classification accuracy of approximately 97%.

5. Architecture Dependent Results and Discussion

After having discussed the epoch dependent development of the training and validation accuracy and loss for the convolutional neural network and the inception architecture for the examples of multi-phase and binary classifiers, we can now shift our interest towards variations of CNN layer numbers, inception blocks and regularization for fine-tuning architectures to achieve maximum prediction accuracies for several different classification tasks involving binary classifiers.

5.1 Isotropic – Nematic/Cholesteric Classification

One of the easiest classification tasks is that between the isotropic and the nematic phase, or for chiral materials that between isotropic and cholesteric, respectively. These are the only machine learning studied transitions in liquid crystals, the reason being that both LC phases display

characteristic defects, topological Schlieren defects and oily streaks for achiral and chiral materials, respectively, which are easy to recognize. The second reason is the fact that this transition very closely resembles that of the texture transition between homeotropic (pseudo-nematic) and planar anchoring conditions as exploited in the automated readout of chemical or biological sensors. In Figure 6 we present the results of the average validation accuracy obtained as a function of the number of CNN layers and different regularization via dropout layers and image flipping for both the achiral and the chiral case.

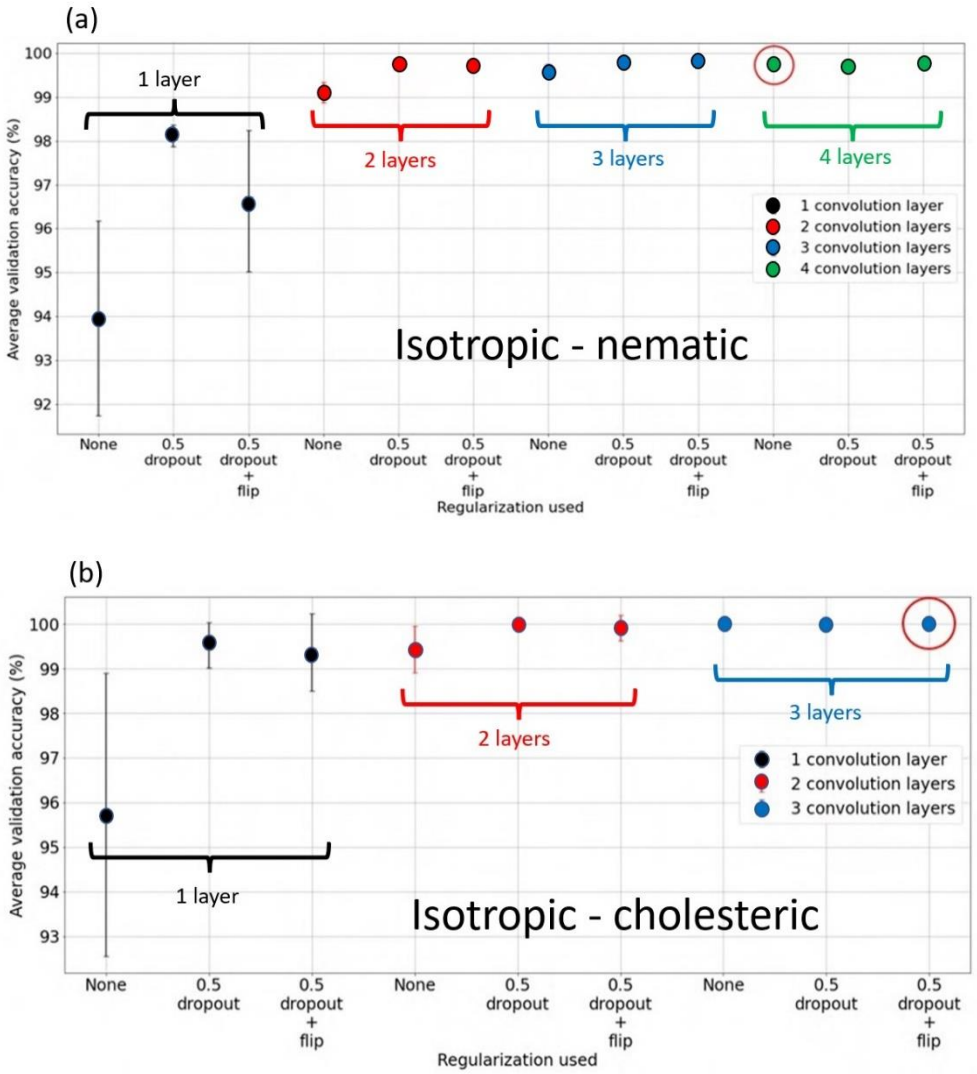

Figure 6: Average validation accuracy for different architectures used in the classification of the (a) isotropic and nematic, as well as (b) the isotropic and chiral nematic / cholesteric liquid crystal phases. Rather independent of the regularization used, it is clear that the architectures approach their maximum accuracy for a certain model complexity beyond a single CNN layer and approaching close to 100% for 3- to 4-layer CNN architectures.

For the isotropic – nematic classification (Figure 6(a)) it is already visually clear that the average validation accuracy approaches its maximum at a 3- or 4-layer CNN architecture. This is largely independent of any regularization used. A single layer CNN architecture is obviously not sufficiently complex to produce adequate results for the classification task, although as can be seen from

Figure 6(a), application of regularization methods already increases the accuracy. The regularizations used here are dropout layers, which apply a mask that nullify the contribution of some neurons to the next layer, leaving all others unchanged, and augmentation methods such as image flipping. A very similar behavior is obtained for the isotropic – cholesteric classification, which is shown in Figure 6(b). For no regularization applied at all, the results can be summarized for these transitions as a quickly increasing validation accuracy with an increasing number of CNN layers, depicted in Figure 7. It should be noted that for further increasing the number of convolutional layers the accuracy may well decrease again, due to overfitting and applying a too complex architecture to the relatively simple classification task.

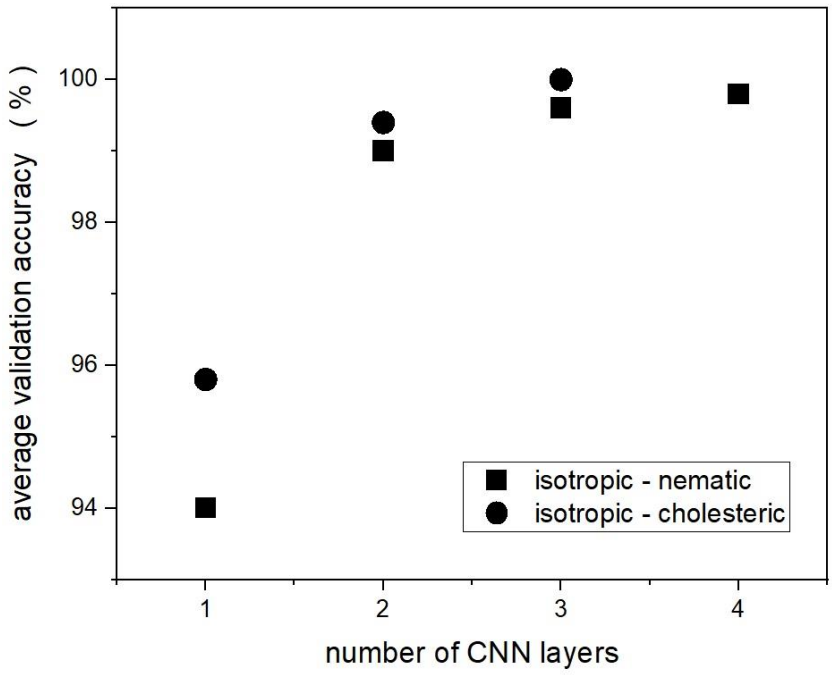

Figure 7: Average validation accuracy as a function of convolutional layers in the CNN architecture. The accuracy quickly approaches 100% for both the isotropic – nematic and the isotropic – cholesteric classification tasks, with no dropout layers or image augmentations applied.

5.2 Nematic/Cholesteric – Smectic Classification

A somewhat more difficult classification task is that between nematic or cholesteric and the fluid smectic phases, and we believe that this has not been investigated besides the studies from our group [30,31]. For this part we chose to employ an inception architecture, varying between one and two inception blocks and applying different regularizations.

Figure 8(a) displays the results for the nematic to smectic classification task as an average validation accuracy (in %) for grouping different regularizations when using a varying number of inception blocks. One can see that on average the architecture with two inception blocks leads to a slightly higher accuracy by approximately 4% when compared to only one inception block, increasing the overall average accuracy from 94% to 98% for the nematic to smectic identification task. At the same time,

variations for individual regularization processes are much reduced. This suggests that the architecture with two inception blocks is more stable and less prone to under and overfitting. This thus appears to be the correct choice of model complexity for the classification task investigated.

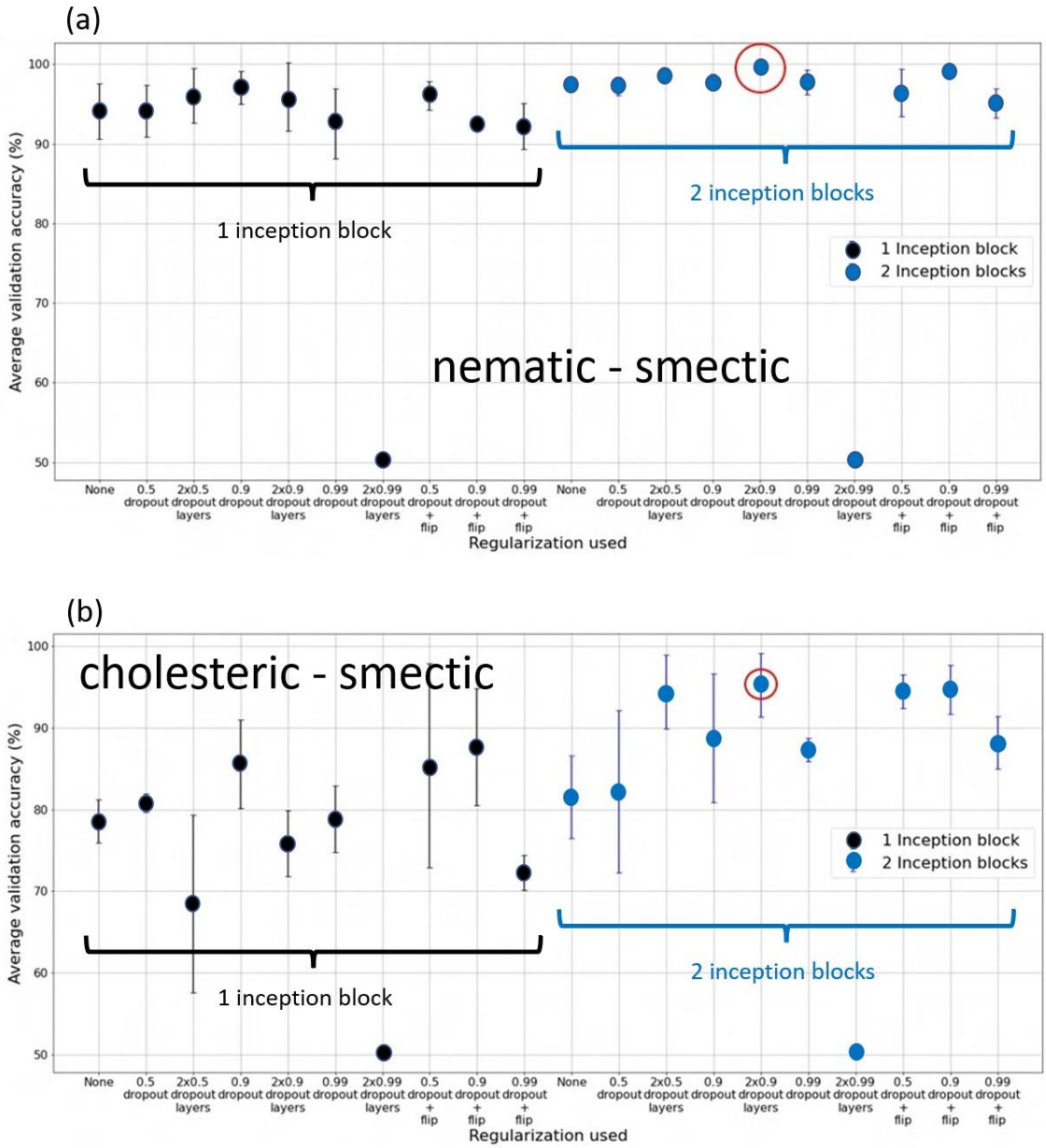

Figure 8: Average validation accuracy for several different regularizations employed on inception architectures with one (black) and two (blue) inception blocks for (a) the nematic to smectic and (b) cholesteric to smectic classification tasks.

A similar, yet more pronounced behavior can be observed for the cholesteric to smectic classification task, with results depicted in Figure 8(b). On average, disregarding different regularizations, the accuracy of the two-inception-block model is about 10% higher than that of the single block architecture, increasing from about 80% to 90%. The second inception block also appears to slightly dampen the variations on different regularization processes. Again, the inception model with two inception blocks appears to have the right complexity for the task investigated. Dropout layers and

flip augmentations then lead to average validation accuracies in the order of 95%, which is absolutely acceptable for this classification task.

5.3 SmA* – SmC* Classification

The classification between smectic A and smectic C on first sight should be a rather complicated task for machine learning, because this is a second order, continuous transition where often only minute changes in texture from a fan-shaped to a broken fan-shaped arrangement are observed. This is certainly true for the transition of an achiral material. We have therefore investigated the chiral version of this transition, smectic A* - smectic C*. This is in most cases still a continuous transition, but at the same time related to the paraelectric to ferroelectric transition, because according to the symmetry arguments by Meyer et al.[44] every tilted smectic phase composed of chiral molecules potentially exhibits a spontaneous polarization P_S and can thus be ferroelectric, if P_S is switchable between two stable states. Due to the fact that the spontaneous polarization vectors would like to compensate in the smallest volume possible, the SmC* phase forms a helical superstructure with the magnitude of the molecular tilt being fixed by thermodynamics, while its direction is free to choose. Due to the coupling between tilt and polarization the molecular helical superstructure is connected to a polarization helix, which compensates P_S over the period of one pitch. The helical superstructure of SmC* in turn gives rise to an equidistant line pattern across the fan-shaped texture, which is distinguishable from the smooth fans of the paraelectric SmA* phase at zero tilt.

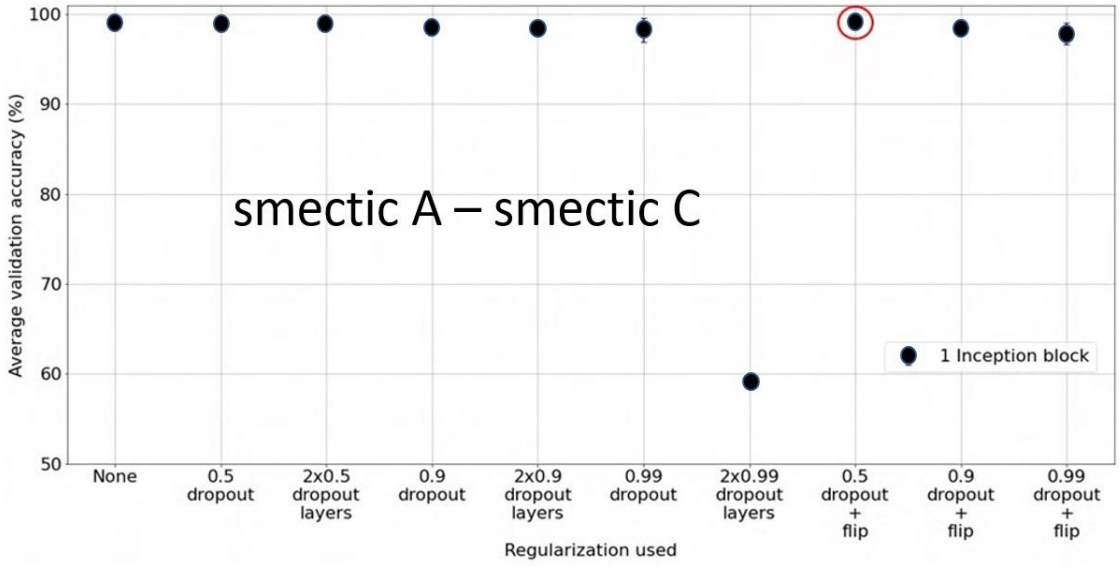

Figure 9: Average validation accuracy for several different regularizations used within a one block inception network architecture to classify between SmA* and SmC*. Accuracies are rather high with values around 99% and nearly independent of regularization. This is due to the fact that in contrast to the achiral SmA-SmC transition, the chiral SmA*-SmC* transition exhibits textures with clearly identifiable differences (see text).

This leads to the observation that the classification task between SmA* and SmC* is much easier and less complex than first anticipated. The results of a single block inception architecture are depicted in Figure 9. It can be seen that, independent of the regularization employed, very high average validation

accuracies of close to 100% are obtained with very little variation (error). This indicates that an inception architecture with a single inception block and no regularization are already sufficient to classify the task with nearly 100% accuracy. Nevertheless, it should be noted that we anticipate the equivalent task carried out for achiral materials to be much harder, involving only minute texture changes and thus require an increased complexity of the machine learning architecture employed.

5.4 Fluid Smectic – Hexatic Classification

Quite a bit harder is the classification of liquid crystal phases when one involves phases of higher order, for example hexatic phases or even soft crystal phases. While we have left the soft crystal phases with their 3D-order for a later investigation, we have studied the classification between phases of fluid to hexatic order. Changes of textures between those two classes of phases are subtle, which is the reason why we employed inception architectures instead of convolutional neural networks. The results of changing from one to two inception blocks, together with regularizations like dropout layers and image flipping augmentations are shown in Figure 10.

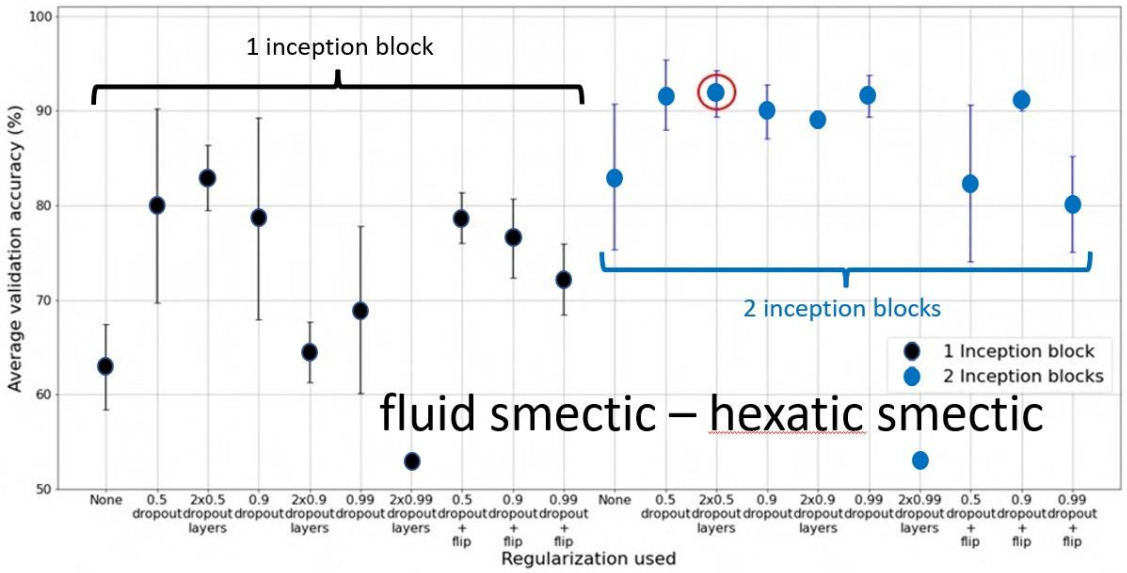

Figure 10: Average validation accuracy for several different regularizations employed on inception architectures with one (black) and two (blue) inception blocks for the fluid smectic to hexatic smectic classification tasks.

One can first of all clearly see that a single inception block architecture is not sufficient to classify between fluid and hexatic smectics with an acceptable accuracy. Comparing architectures without any regularization we obtain 64% average validation accuracy for the single block architecture, which is indeed very close to simply guessing the phases to be classified. The 84% accuracy obtained from the same two-block inception architecture is already quite a bit better and probably in line with a phase characterization done by an experienced researcher, although error margins, i.e. variations in accuracies, are relatively large in both cases. Using regularization methods shows an increase in accuracy for both inception block architectures, especially for employing dropout layers, much less so for flip augmentation. On average over all regularizations, the average validation accuracy

increases from approximately 73% for the one-inception-block architecture to 88% for the two-block inception model. The best result was obtained for an inception architecture with two inception blocks and dropout layer regularization, which gave an average validation accuracy of 92%, a value which is acceptable for such a complex classification task and which we believe would be suitable for large scale automatic phase characterization of liquid crystals.

5.5 Smectic I – Smectic F Classification

As a last classification, we have chosen a rather challenging task in the field of hexatic liquid crystal phases, that of classifying between SmI and SmF, two phases that are only distinguished by the difference of their tilt direction, tilted either towards the apex or the side of the hexagon. Accordingly, the difference between textures of these two phases is mostly minute, thus the complexity of the task is high. Given that from the previous task we knew that satisfying results could most likely be obtained by use of a two or three block inception architecture, we were interested in characterizing how far one could push a conventional CNN by simply increasing the number of layers and applying some regularization, such as dropout layers and flip augmentations. A summary of the results is depicted in Figure 11.

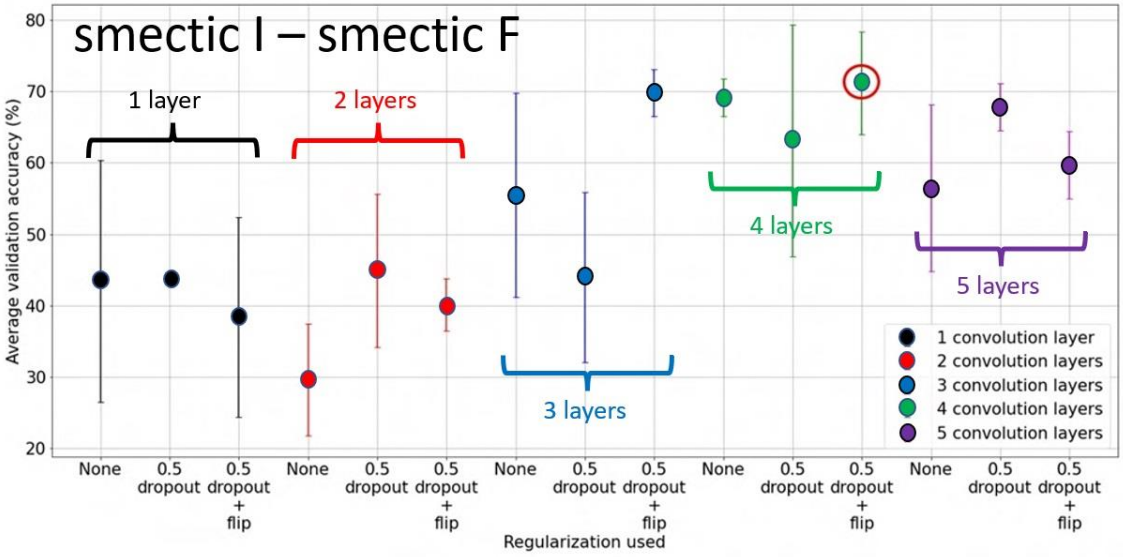

Figure 11: Average validation accuracy as a function of varying regularization for increasing number of CNN layers – thus increasing network architecture complexity.

It should first be noted that this classification task was carried out on the least number of image data input and would thus definitely benefit from an increased image input source which would most likely improve the overall average validation accuracy. Nevertheless, it is also clear that a one or two layer CNN is not sufficiently complex to handle a classification task like this, because the validation accuracy below 50% clearly indicates that this is in the area of guessing, rather than the network learning features to classify the two phases. Increasing the architecture to three and especially four layer CNNs, increases the average validation accuracy by about 30%, which is certainly a step in the right direction, although an accuracy of roughly 70% is still too small to be considered useful in a general

characterization of liquid crystal phases. It is interesting to notice that the validation accuracy decreases again if the architecture is made more complex via the addition of more layers, in this case using a 5-layer CNN architecture. This is an indication of overfitting, which, together with the relatively small amount of image textures, means that the machine learning model is practically starting to learn the textures by heart. The best performing architecture was a 4-layer CNN with dropout layers and flip augmentation, which gave an average validation accuracy of 71%. This is still insufficient for a real liquid crystal characterization tool but provides proof-of-principle that this is indeed possible. To enhance performance, there are several possibilities available: (i) a considerable increase in the number of data input images and (ii) an increase in the complexity of the architecture, for example by using a two- or three-block inception model with regularization. These possibilities do of course imply additional experimental work and longer machine learning training times. The results of this part of the investigation are summarized in Figure 12, showing the average performance over all regularizations as a function of increasing CNN layers.

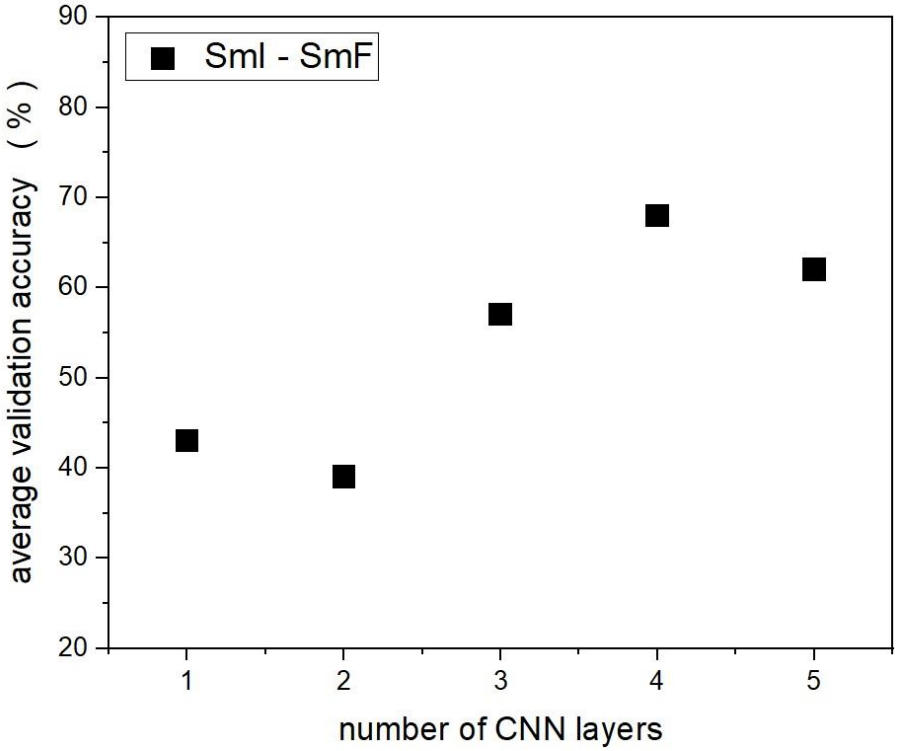

Figure 12: Average validation accuracy as a function of CNN layers over all regularizations and augmentations employed. The network performance increases through 1- to 3- layer CNN architectures to a maximum for 4-layer CNNs and then decreases again. 1- and 2-layer architectures are too simple for the classification task, while at the 5-layer architecture one can see the setting in of overfitting, due to the complexity of the network. Overall, the accuracy values are too small to be of use in the characterization of liquid crystals, which can be accounted for by the small number of data input images for training. Also, for this type of classification task, a two- or three-block inception architecture would most likely be more suitable.

From our recent work [30,31] it has become clear that both convolutional neural networks, as well as inception algorithms, are capable of automatically identifying different phases. This is particularly

valid for phases which exhibit clear differences in textures between phase transitions. For more similar textures a larger number of images is needed and the complexity of the machine learning algorithm needs to be adopted to the complexity of the problem investigated, while paying close attention to avoid overfitting. With these requirements in mind it is in principle possible to identify all known liquid crystal phases, given that the training and validation set of images is large enough. Yet, one does need to keep in mind that phases which exhibit in some cases equivalent textures, for example in series with orthogonal hexatic phases (like SmA and SmB transitions[45]), or in chiral series (like MHPOBC with SmA* and SmC_{α}* transitions[46]), these may not be identified as different phases.

Being a supervised machine learning technique, CNNs and equivalent algorithms as used here, are in principle incapable of predicting novel phases, simply because the signifying features of their textures are not yet known or have not been trained. For example, without any training data in the form of textures, the recently discovered twist-bend nematic phase (N_{TB})[47] or the ferroelectric nematic phase[48] would not be discovered as such. The only indication that a novel phase might be present could possibly be in the form of a low identification accuracy. This would correspond to the attempted identification of a phase which has never been seen before and obviously needs further methodologies. Only after a novel phase is discovered, identified independently, sufficient texture image data is taken and the neural network is trained, can this phase also be identified by supervised machine learning. Nevertheless, even though machine learning is no predictive tool, we believe that the automatic identification of the zoo of already known phases is a large step forward in the characterisation of liquid crystals.

6. Conclusions

A number of different classification tasks of increasing complexity with a range of varied convolutional neural network and inception architectures were investigated. The numbers of layers in CNN models were varied, as were the number of inception blocks. Furthermore, a range of regularization and augmentation procedures were included in the respective network architectures to study their effects on the performance. While for simple classification tasks, like the classification between isotropic and nematic or cholesteric, a 2-layer CNN architecture was already sufficient to yield validation accuracies in excess of 99%, more complex tasks, like the nematic or cholesteric to smectic classification also demanded more complex machine learning models in the form of inception architectures. It was demonstrated that a single inception block is generally not sufficient to produce adequate accuracies and one needs to resort to 2-block inception architectures to increase accuracies. These accuracies may further be increased by applying regularization and augmentation procedures like dropout layers and image flipping. The latter measures can reduce overfitting and artificially increase the training data, respectively. It was demonstrated that classification between fluid and hexatic smectics is possible, even between different hexatic phases to some extent. The latter classification task

somewhat suffered from the lack of sufficient input data but at least provided proof-of-principle results.

In conclusion, provided that sufficient input data and a balanced dataset is available for all liquid crystalline phases, together with sufficient computational resources, we have provided evidence and a pathway via machine learning that automatic phase sequence determination would be possible. From the presented results, the pathway will depend on the complexity of the classification task. For simple phase sequences, for instance Iso-N-Cryst, Iso-SmA-Cryst, or Iso-N-SmA-Cryst a 2- or 3-layer CNN architecture would probably be sufficient to classify the whole sequence with very good accuracy larger than 95%. For more complex phase sequences, for instance Iso-N*-SmA*-SmC*-SmI*-SmF*-Cryst, or Iso-N-SmA-SmB-SmE-Cryst, an inception architecture with two or three inception blocks and regularization via dropout layers would most likely be required. In any case, one would need to match the complexity of the machine learning architecture with that of the classification task and closely monitor for under- or overfitting.

References

[1] Collings PJ, Goodby JW. Introduction to Liquid Crystals: Chemistry and Physics 2nd ed. Boca Raton: CRC Press; 2020.

[2] Singh S. Liquid Crystals: Fundamentals. Singapore: World Scientific Publishing; 2002.

[3] Dierking I. Textures of Liquid Crystals. Weinheim: Wiley-VCH; 2003.

[4] Kumar S (ed.). Liquid Crystals: Experimental Study of Physical Properties and Phase Transitions. Cambridge: Cambridge University Press; 2000.

[5] Sigaki HYD, Lenzi EK, Zola RS, Perc M, Ribeiro HV. Learning physical properties of liquid crystals with deep convolutional neural networks. Sci. Rep. 2020; 10: 7664.

[6] Sigaki HYD, de Souza RF, de Souza RT, Zola RS, Ribeiro HV. Estimating physical properties from liquid crystal textures via machine learning and complexity-entropy methods. Phys. Rev. E. 2019; 99: 013311.

[7] Butler KT, Davies DW, Cartwright H, Isayev O, Walsh A. Machine learning for molecular and materials science. Nature. 2018; 559: 547.

[8] Schmidt J, Marques MRG, Botti S, Marques MAL. Recent advances and applications of machine learning in solid state materials science. NPJ Comp. Mat. 2019; 5: 83.

[9] Jackson NE, Webb MA, de Pablo JJ. Recent advances in machine learning towards multiscale soft materials design. Current Opinion in Chem. Eng. 2019; 23: 106.

[10] Pessa AAB, Zola RS, Perc M, Ribeiro HV. Determining liquid crystal properties with ordinal networks and machine learning. Chaos, Solitons and Fractals. 2022; 154: 111607.

[11] Chen C-H, Tanaka K, Funatsu K. Random Forest Model with Combined Features: A Practical Approach to Predict Liquid-crystalline Property. Mol. Inf. 2019; 38: 1800095.

[12] Inokuchi T, Okamoto R, Arai N. Predicting molecular ordering in a binary liquid crystal using machine learning. Liq. Cryst. 2020; 47: 438.

[13] Le TC, Tran N. Using Machine Learning to Predict the Self-Assembled Nanostructures of Monoolein and Phytantriol as a Function of Temperature and Fatty Acid Additives for Effective Lipid-Based Delivery Systems. ACS Appl. Nano Mater. 2019; 2: 1637.

[14] Walters M, Wei Q, Chen JZY. Machine learning topological defects of confined liquid crystals in two dimensions. Phys. Rev. E. 2019; 99: 062701.

[15] Minor EN, Howard SD, Green AAS, Glaser MA, Park CS, Clark NA. End-to-end machine learning for experimental physics: using simulated data to train a neural network for object detection in video microscopy. Soft Matter. 2020; 16: 1751.

[16] Colen J, Han M, Zhang R, Redford SA, Lemma LM, Morgan L, Ruijgrok PV, Adkins R, Bryant Z, Dogic Z, Gardel ML, de Pablo JJ, Vitelli V. Machine learning active-nematic hydrodynamics. PNAS. 2021; 118: e2016708118.

[17] Hedlund E, Hedlund K, Green A, Chowdhury R, Park CS, Maclennan JE, Clark NA. Detection of islands and droplets on smectic films using machine learning. Phys. Fluids. 2022; 34: 103608.

[18] He W-L, Cui Y-F, Luo S-G, Hu W-T, Wang K-N, Yang Z, Cao H, Wang D. High-Throughput Preparation and Machine Learning Screening of a Blue-Phase Liquid Crystal Based on Inkjet Printing. Molecules. 2022; 27: 6938.

[19] Zhang Y-G, Cui Y-F, Hao W, Wan-li HE, Zhang L, Yang Z, Cao H, Wang D, Li Y-Z. High-throughput blue phase liquid crystal recognition based on convolutional neural network. Chinese J. Liq. Cryst. and Displays. 2022; 36: 972.

[20] Nayani K, Yang Y, Yu H, Jani P, Mavrikakis M, Abbott NL. Areas of opportunity related to design of chemical and biological sensors based on liquid crystals. Liq. Cryst. Today. 2020; 29: 24.

[21] Cao Y, Yu H, Abbott NL, Zavala VM. Machine Learning Algorithms for Liquid Crystal-Based Sensors. ACS Sens. 2018; 3: 2237.

[22] Bao N, Jiang S, Smith A, Schauer JJ, Mavrikakis M, van Lehn RC, Zavala VM, Abbott NL. Sensing Gas Mixtures by Analyzing the Spatiotemporal Optical Responses of Liquid Crystals Using 3D Convolutional Neural Networks. ACS Sens. 2022; 7: 2545.

[23] Ramou E, Palma SICJ, Roque ACA. Nanoscale Events on Cyanobiphenyl-Based Self-Assembled

Droplets Triggered by Gas Analytes. ACS Appl. Mater. Interfaces. 2022; 14: 6261.

[24] Xu Y, Rather AM, Song S, Fang J-C, Dupont RL, Kara UI, Chang Y, Paulson JA, Qin R, Bao X, Wang X. Ultrasensitive and Selective Detection of SARS-CoV-2 Using Thermotropic Liquid Crystals and Image-Based Machine Learning. Cell Rep. Phys. Sci. 2020; 1: 100276.

[25] Jiang S, Noh JH, Park C, Smith AD, Abbott NL, Zavala VM. Using machine learning and liquid crystal droplets to identify and quantify endotoxins from different bacterial species. Analyst. 2021; 146: 1224.

[26] Matysiewicz M, Neumann T, Nowak RM, Okuniewski R, Oleszkiewicz W, Cichosz P, Jagodziński D. Automatic recognition of thermographic examinations for early detection of breast cancer. Proc. SPIE 10031, Photonics Applications in Astronomy, Communications, Industry, and High-Energy Physics Experiments. 2016; 100312X, https://doi.org/10.1117/12.2249067.

[27] Kang SB, Lee JH, Song KY, Pahk HJ. Automatic Defect Classification of TFT-LCD Panels Using Machine Learning. IEEE International Symposium on Industrial Electronics (ISlE 2009) Seoul Olympic Parktel, Seoul, Korea July 5-8. 2009; 2175.

[28] Zuvela P, Lovric M, Yousefian-Jazi A, Liu JJ. Ensemble Learning Approaches to Data Imbalance and Competing Objectives in Design of an Industrial Machine Vision System. Ind. Eng. Chem. Res. 2020; 59: 4636.

[29] Liu Y, Lu H-P, Lai C-H. A Novel Attention-Based Multi-Modal Modeling Technique on Mixed Type Data for Improving TFT-LCD Repair Process. IEEE Access. 2022; 10: 33026.

[30] Dierking I, Dominguez J, Harbon J, Heaton J. Classification of liquid crystal textures using convolutional neural networks. Liq. Cryst. 2022; https://doi.org/10.1080/02678292.2022.2150790

[31] Dierking I, Dominguez J, Harbon J, Heaton J. Deep Learning techniques for the localization and classification of liquid crystal phase transitions. Frontiers in Soft Matter. 2023; 3: 1114551.

[32] Goodfellow I, Bengio Y, Courville A. Deep Learning. Cambridge (MA): MIT Press; 2016.

[33] Murphy KP. Machine Learning: A Probabilistic Perspective. Cambridge (MA): The MIT Press; 2015.

[34] Mitchell TM, Machine learning. New York (NY): WCB/McGraw-Hill; 1997.

[35] Kingma DP, Adam JB: A method for stochastic optimization. 2017. arXiv preprint arXiv:1412.6980, 2014 - arxiv.org

[36] Lever J, Krzywinski M, Altman N. Model selection and overfitting. Nature Methods. 2016; 13: 703.

[37] Lecun Y, Bottou L, Bengio Y, Haffner P. Gradient-based learning applied to document recognition. Proc. of the IEEE. 1998; 86: 2278.

[38] Szegedy C, Liu W, Jia Y, Sermanet P, Reed S, Anguelov D, Erhan D, Vanhoucke V, Rabinovich A. Going deeper with convolutions. CoRR; abs/1409.4842, 2014. [Online]. Available: http://arxiv.org/abs/1409.4842.

[39] Dierking I, Giesselmann F, Kusserow J, Zugenmaier P. Properties of higher-ordered ferroelectric liquid crystal phases of a homologues series. Liq. Cryst. 1994; 17: 243.

[40] Schacht J, Dierking I, Giesselmann F, Mohr K, Zaschke H, Kuczynski W, Zugenmaier P. Mesomorphic properties of a homologues series of chiral liquid crystals containing the α-chloroester group. Liq. Cryst. 1995; 19: 151.

[41] "VideoLAN VLC media player," https://www.videolan.org/vlc/

[42] "Keras API," https://keras.io/.

[43] "Google Colaboratory," https://colab.research.google.com/.

[44] Meyer RB, Liebert L, Strzelecki L, Keller P. Ferroelectric liquid crystals. J. de Phys. Lett. 1975; 36: 69

[45] Betts R, Dierking I. in preparation

[46] Betts R, Dierking I. in preparation

[47] Imrie CT, Walker R, Storey JMD, Gorecka E, Pociecha D. Liquid Crystal Dimers and Smectic Phases from the Intercalated to the Twist-Bend. Crystals. 2022; 12: 1245.

[48] Chen X, Korblova E, Dong D, Wei X, Shao R, Radzihovsky L, Glaser M, Maclennan J, Bedrov D, Walba D, Clark NA. First-Principles Experimental Demonstration of Ferroelectricity in a Thermotropic Nematic Liquid Crystal: Spontaneous Polar Domains and Striking Electro-Optics. PNAS. 2020; 117: 14021.

Graphical abstract

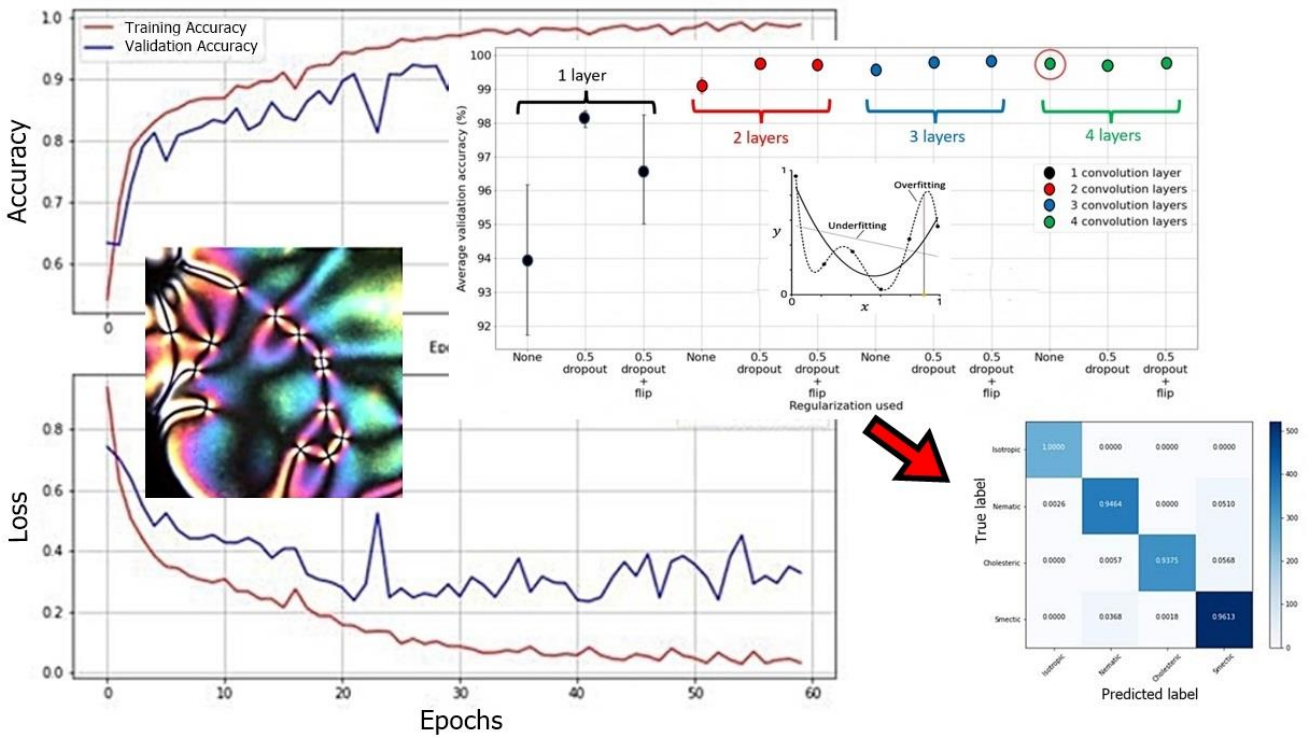

Different convolutional neural network and inception network architectures were trained for the classification of liquid crystal phases through textures to test the prediction accuracy for each one of these models varying the number of layers, inception blocks and regularization methods.